# Optical angular momentum transfer on total internal reflection

ATIRACH RITBOON[1,*], SARAH CROKE[1], AND STEPHEN M BARNETT[1]

[1] School of Physics and Astronomy, University of Glasgow, Glasgow G12 8QQ, UK
[*] Corresponding author: a.ritboon.1@research.gla.ac.uk

Compiled January 30, 2019

**We study the mechanism of optical angular momentum transfer from light to a dielectric medium on total internal reflection. We employ a quantized approach and, in particular, work with a single-photon pulse. This allows us to evaluate the force and torque per photon and also, crucially, to evaluate forces and torques conditioned on transmission or reflection at an interface. The reflected electric and magnetic fields of an incident paraxial beam carrying orbital and spin angular momentum are obtained using an angular spectrum method. We calculate the expectation value of the single-photon torque exerted on the dielectric, due to total internal reflection of a single-photon pulse, using the dipole-based Lorentz force density. We apply this result to describe the angular momentum transfer from light on passing through an M-shaped Dove prism.** 

http://dx.doi.org/10.1364/ao.XX.XXXXXX

## 1. INTRODUCTION

It is now well-established that light can carry both spin **S** [1], and also orbital angular momentum **L** [2]. In the paraxial regime, the spin and orbital angular momentum are associated with circular polarization and helically-phased spatial modes respectively. A beam in a Laguerre-Gaussian (LG) mode with azimuthal phase term $e^{il\phi}$ carries $\hbar l$ units of orbital angular momentum per photon in free space. Some care is needed as, more generally, neither the spin nor the orbital angular momentum alone can represent a true angular momentum, only the total angular momentum, $\mathbf{J} = \mathbf{S} + \mathbf{L}$, is a true angular momentum [3–5]. However, each is separately measurable, as shown in many experiments, and also separately conserved, as they correspond to different symmetries [6, 7].

In this work, we study the mechanism of angular momentum transfer from a single-photon pulse to a lossless dielectric medium by using the dipole-based force density [8, 9]. Working directly with the force bypasses the need to specify the momentum of the photon and hence avoids the subtle issues associated with the much-discussed Abraham-Minkowski dilemma [10–12].

For definiteness, we consider our incident photon to be in an LG mode with zero radial index. The dielectric medium size is taken to be very large compared to the pulse length so that we can isolate the effects of transmission through or reflection from interfaces. The incident beam is assumed to be a paraxial single-photon pulse with narrow-bandwidth spectrum, so that each of the quantities reported here are normalized for one photon. The central wavelength of the photon is assumed to be much smaller than its beam waist. The physical results presented might be obtained, with effort, from classical electrodynamics. A quantum calculation has the key advantage, however, that we can eliminate the complications due to the coexistence of reflection and transmission at an interface by conditioning the forces and torques on the transmission or reflection of the photon. This greatly simplifies the analysis and also clarifies the physical interaction. Moreover, the quantum calculation allows us to express the physical quantities obtained in units of per photon.

In section 2, we present the angular spectrum representation as an important ingredient used to determine the form of the reflected beam. We apply the regular quantization procedure to promote the classical fields to the corresponding field operators. We then give, in section 3, a discussion of total force and total torque in the case that there is an interface involved. In section 4, the form of the total torque given in section 3 is used to evaluate the effective torque exerted by the single-photon pulse to the dielectric medium, and the angular momentum transfer. Section 5 then focuses on the transfer of angular momentum from a single photon to an M-shaped Dove prism.

## 2. ANGULAR SPECTRUM REPRESENTATION AND FIELD QUANTIZATION

### A. Angular representation

In this section, we will start by introducing the angular spectrum representation. For a paraxial beam with finite cross-section, the Lorenz-gauge vector potential of the electromagnetic wave of frequency $\omega$ traveling in the $z$ direction in a dielectric with

refractive index $n(\omega)$ will be of the form [13]

$$\mathbf{A}(\mathbf{r},t) = A_0(\alpha\mathbf{x}+\beta\mathbf{y})u_{k,l}(x,y,z)\mathrm{e}^{-\mathrm{i}\omega t+\mathrm{i}kz}, \tag{1}$$

where $A_0$ is a complex constant, $\mathbf{x}$ and $\mathbf{y}$ are unit vectors in the positive x and y directions respectively, $k = n(\omega)\omega/c$, and the complex constants $\alpha$ and $\beta$, with $|\alpha|^2+|\beta|^2 = 1$, determine the polarization. As we are working in a lossless medium, the refractive index, $n(\omega)$, is a real number. To simplify the calculation, we restrict ourselves to the simplest form of Laguerre-Gaussian modes by considering only the case when the radial index $p = 0$, and the complex scalar function in Cartesian coordinates is given as [2, 13]

$$\begin{aligned} u_{k,l}(x,y,z) =& \sqrt{\frac{2}{\pi\,|l|!w^2(z)}}\left(\frac{\sqrt{2}(x+\mathrm{i}\,\mathrm{sign}(l)y)}{w(z)}\right)^{|l|} \\ &\times\exp\left[-\left(\frac{1}{w^2(z)}-\frac{\mathrm{i}kz}{2(z^2+z_\mathrm{R}^2)}\right)(x^2+y^2)\right] \\ &\times\exp[-\mathrm{i}(|l|+1)\tan^{-1}(z/z_\mathrm{R})] \\ \approx& \frac{1}{\sqrt{\pi|l|!}}\left(\frac{\sqrt{2}}{w_0}\right)^{|l|+1}(x+\mathrm{sign}(l)\mathrm{i}y)^{|l|} \\ &\times\exp\left[-\left(\frac{1}{w_0^2}-\frac{\mathrm{i}kz}{2z_\mathrm{R}^2}\right)(x^2+y^2)-\mathrm{i}(|l|+1)\frac{z}{z_\mathrm{R}}\right], \end{aligned} \tag{2}$$

where $l$ is an orbital angular-momentum quantum number, or a topological charge and the Rayleigh range is denoted by $z_\mathrm{R}$, which is related to the beam waist $w_0$ as $z_\mathrm{R} = kw_0^2/2$. The origin of the coordinates is placed at the position of the waist. Our approximation is valid only in the range of $z \ll z_\mathrm{R}$, and in this work we will focus, for simplicity, only in this region of $z$. The mode function is normalized such that the integration of its strength over the $xy$- plane is unity:

$$\int_{-\infty}^{\infty}\int_{-\infty}^{\infty}\mathrm{d}x\mathrm{d}y\,|u_{k,l}(x,y,z)|^2 = 1, \tag{3}$$

where

$$|u_{k,l}(x,y,z)|^2 = \frac{2^{|l|+1}}{\pi|l|!w_0^{2(|l|+1)}}(x^2+y^2)^{|l|}\exp(-2(x^2+y^2)/w_0^2). \tag{4}$$

The paraxial regime implies that the beam waist is much larger than the wavelength, in other words, $kw_0 \gg 1$. The spin angular momentum quantum number of the beam, denoted by $\sigma$, can be calculated by the given polarization coefficients in Eq. 1 as [2, 14]

$$\sigma = \mathrm{i}(\alpha\beta^* - \alpha^*\beta), \tag{5}$$

which correspond to $\pm1$ for right and left circular polarizations and 0 for linear polarization.

An electromagnetic beam may be expressed as a superposition of plane waves whose amplitudes and propagation directions are varied. This indicates that each plane wave component of the beam will hit the interface with a different incident angle and also have its own plane of incidence. The angular spectrum representation thus significantly helps us to determine both the transmitted and reflected beams. Within the paraxial approximation the two dimensional Fourier transform of the vector potential in an LG mode is

$$\begin{aligned} \mathbf{A}(\mathbf{r},t) =& (\alpha\mathbf{x}+\beta\mathbf{y})\mathrm{e}^{-\mathrm{i}\omega t+\mathrm{i}kz}\frac{A_0}{(2\pi)^2} \\ &\times\int_{-\infty}^{\infty}\int_{-\infty}^{\infty}\mathrm{d}k_x\mathrm{d}k_y\tilde{u}_l(k_x,k_y)\mathrm{e}^{-\mathrm{i}z(k_x^2+k_y^2)/2k}\mathrm{e}^{\mathrm{i}(k_xx+k_yy)}, \end{aligned} \tag{6}$$

where

$$\tilde{u}_l(k_x,k_y) \propto (\mathrm{sign}(l)\mathrm{i}k_x - k_y)^{|l|}\exp\left[-\frac{(k_x^2+k_y^2)w_0^2}{4}\right], \tag{7}$$

and the paraxial approximation $k_z \approx k-(k_x^2+k_y^2)/2k$ has been applied. The transverse components of the wave vector are much smaller than the wave vector magnitude: $k_\perp \ll k$, where we denote $k_\perp$ as the wave vector components in the transverse directions, which are $k_x$ and $k_y$ in this case. The positive-frequency electric and magnetic fields in the Lorenz gauge can then be obtained from the given vector potential $\mathbf{A}$ as [15]

$$\begin{aligned} \mathbf{E}(\mathbf{r},t) =& -\nabla\phi(\mathbf{r},t) - \frac{\partial\mathbf{A}(\mathbf{r},t)}{\partial t}, \\ =& \mathrm{i}\frac{c^2}{\omega n^2}\nabla(\nabla\cdot\mathbf{A}(\mathbf{r},t)) + \mathrm{i}\omega\mathbf{A}(\mathbf{r},t) \\ =& \mathrm{e}^{\mathrm{i}(kz-\omega t)}\frac{A_0}{(2\pi)^2}\int_{-\infty}^{\infty}\int_{-\infty}^{\infty}\mathrm{d}k_x\mathrm{d}k_y\tilde{u}_l(k_x,k_y)\mathrm{e}^{-\mathrm{i}z(k_x^2+k_y^2)/2k} \\ &\times\left\{\mathrm{i}\omega(\alpha\mathbf{x}+\beta\mathbf{y}) - \frac{\mathrm{i}c}{n}(\alpha k_x+\beta k_y)\mathbf{z}\right\}\mathrm{e}^{\mathrm{i}(k_xx+k_yy)}, \\ \approx& A_0\left\{\mathrm{i}\omega(\alpha\mathbf{x}+\beta\mathbf{y})u_{k,l} - \frac{c}{n}\mathbf{z}\left(\alpha\frac{\partial u_{k,l}}{\partial x}+\beta\frac{\partial u_{k,l}}{\partial y}\right)\right\}\mathrm{e}^{\mathrm{i}(kz-\omega t)}, \end{aligned} \tag{8}$$

$$\begin{aligned} \mathbf{B}(\mathbf{r},t) =& \nabla\times\mathbf{A}(\mathbf{r},t), \\ =& \mathrm{e}^{\mathrm{i}(kz-\omega t)}\frac{A_0}{(2\pi)^2}\int_{-\infty}^{\infty}\int_{-\infty}^{\infty}\mathrm{d}k_x\mathrm{d}k_y\tilde{u}_l(k_x,k_y)\mathrm{e}^{-\mathrm{i}z(k_x^2+k_y^2)/2k} \\ &\times\left\{\frac{-\mathrm{i}\omega n}{c}(\beta\mathbf{x}-\alpha\mathbf{y}) + \mathrm{i}(\beta k_x-\alpha k_y)\mathbf{z}\right\}\mathrm{e}^{\mathrm{i}(k_xx+k_yy)}, \\ \approx& A_0\left\{-\mathrm{i}k(\beta\mathbf{x}-\alpha\mathbf{y})u_{k,l} + \mathbf{z}\left(\beta\frac{\partial u_{k,l}}{\partial x}-\alpha\frac{\partial u_{k,l}}{\partial y}\right)\right\}\mathrm{e}^{\mathrm{i}(kz-\omega t)}, \end{aligned} \tag{9}$$

where the paraxial approximation has been applied: the terms that are of order $(k_\perp)^2/k$ or higher are omitted as they only give extremely small contributions compared to the first order terms. The last lines of Eq. 8 and Eq. 9 are the fields in real space after the inverse Fourier transform has been applied. We note that, in contrast to the case of a plane wave, there are electric and magnetic fields in the direction of propagation. However, these fields still obey Maxwell's equations for the source-free case: $\nabla\cdot\mathbf{E} = 0$ and $\nabla\cdot\mathbf{B} = 0$. The $z$ components of the electric and magnetic fields are much smaller than their $x$ and $y$ components, which can be seen in their angular spectrum representations.

### B. Reflected field calculation

As we are focusing on the case of total internal reflection, this subsection will demonstrate how one can determine the reflected field using the angular spectrum representation and the physics of reflection of plane waves. As mentioned earlier, an electromagnetic beam is a superposition of plane waves, and these plane waves hit the interface differently. With the help of the

angular spectrum representation in the previous subsection, we can determine the reflected fields for each plane wave individually and sum these up later to determine the reflected beam as desired. Figure 1 presents three different local coordinate systems: incident, reflected and interface coordinates denoted by $(x_\mathrm{i}, y_\mathrm{i}, z_\mathrm{i})$, $(x_\mathrm{r}, y_\mathrm{r}, z_\mathrm{r})$ and $(x, y, z)$ respectively. We suppose that the interface plane is located at $z = 0$ and the dielectric medium occupies in the region $z < 0$ as depicted in the figure. The unit vectors of these coordinates are as depicted in the figure, but to simplify the calculation we let the origins of those coordinates be located at the same point, at the origin of the coordinates $(x, y, z)$. The unit vectors $\mathbf{y}_\mathrm{i}$, $\mathbf{y}_\mathrm{r}$ and $\mathbf{y}$ are pointing into the same direction.

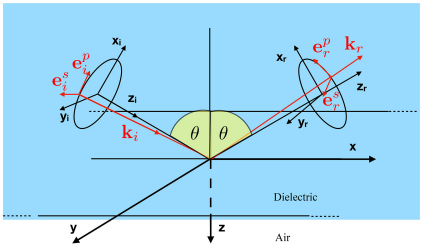


**Fig. 1.** The geometrical alignment of incident, reflected and interface coordinates is illustrated, and these coordinates share the same origin point. The red line shows the propagation path of the local plane wave with the incident wave vector $\mathbf{k}_\mathrm{i}$. The local wave vector and the local polarizations form a local Cartesian coordinate system.

We suppose that the incident field is in an LG mode as previously discussed, and it is in the form given in Eq. 8 but written in the incident coordinates, $(x_\mathrm{i}, y_\mathrm{i}, z_\mathrm{i})$. The position of the incident beam waist is at the origin. However, to directly apply the reflection law, it is convenient to use the interface coordinates $(x, y, z)$. The coordinate transformation between $(x_\mathrm{i}, y_\mathrm{i}, z_\mathrm{i})$ and $(x, y, z)$ coordinates can be expressed as

$$\begin{aligned} x_\mathrm{i} &= x\cos\theta - z\sin\theta, \\ y_\mathrm{i} &= y, \\ z_\mathrm{i} &= z\cos\theta + x\sin\theta. \end{aligned} \tag{10}$$

The electric field of the incident beam in the interface coordinates is then

$$\mathbf{E}_\mathrm{i}(x, y, z, t) = \frac{1}{(2\pi)^2}\int_{-\infty}^{\infty}\int_{-\infty}^{\infty} \mathrm{d}k_x \mathrm{d}k_y \mathbf{E}_\mathrm{i}(k_x, k_y, t), \tag{11}$$

with

$$\begin{aligned} \mathbf{E}_\mathrm{i}(k_x, k_y, t) \equiv & A_0 \mathrm{e}^{-\mathrm{i}\omega t}\left\{\left(\mathrm{i}\omega\alpha\cos\theta - \frac{\mathrm{i}c}{n}(\alpha k_x + \beta k_y)\sin\theta\right)\mathbf{x} + \right. \\ & \mathrm{i}\omega\beta\mathbf{y} - \left.\left(\mathrm{i}\omega\alpha\sin\theta + \frac{\mathrm{i}c}{n}(\alpha k_x + \beta k_y)\cos\theta\right)\mathbf{z}\right\} \\ & \times \tilde{u}_l(k_x, k_y)\mathrm{e}^{\mathrm{i}\mathbf{k}_\mathrm{i}\cdot\mathbf{r}} \end{aligned} \tag{12}$$

and $\mathbf{k}_\mathrm{i} = ((k-\kappa)\sin\theta + k_x\cos\theta, k_y, (k-\kappa)\cos\theta - k_x\sin\theta)$ where $\kappa = (k_x^2 + k_y^2)/2k$. The electric field of the incident beam $\mathbf{E}_\mathrm{i}(x, y, z, t)$ is now in the form of a superposition of plane waves. Therefore, $\mathbf{E}_\mathrm{i}(k_x, k_y, t)$ can be thought of as a local plane wave because it represents a plane wave component in the superposition. Note that $k_x$ and $k_y$ are regarded as the components in the $x_\mathrm{i}$ and $y_\mathrm{i}$ direction of the local wave vector in the incident frame. However, their physical meanings at the interface frame $(x, y, z)$ are difficult to picture, so at this point we treat $k_x$ and $k_y$ as the transform variables. We are then ready to calculate the reflected beam.

Let us consider the plane wave $\mathbf{E}_\mathrm{i}(k_x, k_y, t)$ traveling with its own wave vector $\mathbf{k}_\mathrm{i}$ in the interface coordinates. As this plane wave has its own plane of incidence, two local eigenpolarizations for this local plane wave are expected, and we denote $\mathbf{e}^\mathrm{s}(\mathbf{k}_\mathrm{i})$ and $\mathbf{e}^\mathrm{p}(\mathbf{k}_\mathrm{i})$ as the unit vectors for those local polarizations. The superscripts s and p are used to indicate the polarizations perpendicular and parallel to the local plane of incidence. The local plane of incidence generally is defined as the plane that the normal vector of the interface $\mathbf{n}$ and the local wave vector lie in. In this case, the normal vector is the unit vector $\mathbf{z}$. The local polarization $\mathbf{e}^\mathrm{s}(\mathbf{k}_\mathrm{i})$ can thus be defined as

$$\mathbf{e}^\mathrm{s}(\mathbf{k}_\mathrm{i}) = \frac{\mathbf{z}\times\mathbf{k}_\mathrm{i}}{|\mathbf{z}\times\mathbf{k}_\mathrm{i}|}, \tag{13}$$

and the unit vector which is parallel to the local plane of incidence will then be

$$\mathbf{e}^\mathrm{p}(\mathbf{k}_\mathrm{i}) = \frac{\mathbf{e}^\mathrm{s}(\mathbf{k}_\mathrm{i})\times\mathbf{k}_\mathrm{i}}{k}. \tag{14}$$

The electric field of the local plane wave can now be written in terms of these unit vectors as

$$\mathbf{E}_\mathrm{i}(k_x, k_y, t) = \left\{E_\mathrm{i}^\mathrm{s}(\mathbf{k}_\mathrm{i})\mathbf{e}^\mathrm{s}(\mathbf{k}_\mathrm{i}) + E_\mathrm{i}^\mathrm{p}(\mathbf{k}_\mathrm{i})\mathbf{e}^\mathrm{p}(\mathbf{k}_\mathrm{i})\right\} e^{-\mathrm{i}\omega t + \mathrm{i}\mathbf{k}_\mathrm{i}\cdot\mathbf{r}}, \tag{15}$$

where $E_\mathrm{i}^\mathrm{s}(\mathbf{k}_\mathrm{i}) = \mathbf{E}_\mathrm{i}(k_x, k_y, t)\cdot\mathbf{e}^\mathrm{s}(\mathbf{k}_\mathrm{i})e^{\mathrm{i}\omega t - \mathrm{i}\mathbf{k}_\mathrm{i}\cdot\mathbf{r}}$ and $E_\mathrm{i}^\mathrm{p}(\mathbf{k}_\mathrm{i}) = \mathbf{E}_\mathrm{i}(k_x, k_y, t)\cdot\mathbf{e}^\mathrm{p}(\mathbf{k}_\mathrm{i})\mathrm{e}^{\mathrm{i}\omega t - \mathrm{i}\mathbf{k}_\mathrm{i}\cdot\mathbf{r}}$, and $\mathbf{r}$ is the position vector in the interface coordinates $(x, y, z)$.

The propagation direction of the reflected and transmitted fields of this local plane wave can be determined directly by the law of reflection and Snell's law. The components of wave vectors parallel to the interface are unchanged after transmission and reflection:

$$k_x^\mathrm{i} = k_x^\mathrm{r} = k_x^\mathrm{t}, \qquad \text{and} \qquad k_y^\mathrm{i} = k_y^\mathrm{r} = k_y^\mathrm{t}, \tag{16}$$

and the components perpendicular to the interface are

$$\begin{aligned} k_z^\mathrm{t} &= \sqrt{|\mathbf{k}_\mathrm{t}|^2 - (k_x^\mathrm{t})^2 - (k_y^\mathrm{t})^2} = \sqrt{|\mathbf{k}_\mathrm{t}|^2 - (k_x^\mathrm{i})^2 - (k_y^\mathrm{i})^2}, \\ k_z^\mathrm{r} &= -k_z^\mathrm{i}, \end{aligned} \tag{17}$$

where $k_\gamma^\mathrm{i}$, $k_\gamma^\mathrm{r}$ and $k_\gamma^\mathrm{t}$ are the components of the wave vectors of the incident plane wave, $\mathbf{k}_\mathrm{i}$, its corresponding reflected plane wave, with wave vector $\mathbf{k}_\mathrm{r}$, and its transmitted plane wave, with wave vector $\mathbf{k}_\mathrm{t}$, in $\gamma$ directions when $\gamma = x, y, z$. The magnitudes of those waves are related by the fact that the frequency of the field is not changed by reflection or transmission:

$$\frac{|\mathbf{k}_\mathrm{i}|}{n_\mathrm{i}} = \frac{|\mathbf{k}_\mathrm{t}|}{n_\mathrm{t}} = \frac{\omega}{c}, \tag{18}$$

where $n_\mathrm{i}$ and $n_\mathrm{t}$ are used to represent the refractive indices of the media where the wave is propagating from and transmitted through. As plane waves in the superposition of Eq. 11 hit the interface with different angles, their corresponding transmission and reflection coefficients of the two local eigenpolarizations vary with their particular incident angles, in other words they

depend on the propagation of the local incident plane wave [16]:

$$t^{\mathrm{s}}(k_x,k_y) = \frac{2k_z^{\mathrm{i}}}{k_z^{\mathrm{i}}+k_z^{\mathrm{t}}}, \tag{19a}$$

$$r^{\mathrm{s}}(k_x,k_y) = \frac{k_z^{\mathrm{i}}-k_z^{\mathrm{t}}}{k_z^{\mathrm{i}}+k_z^{\mathrm{t}}}, \tag{19b}$$

$$t^{\mathrm{p}}(k_x,k_y) = \frac{2nk_z^{\mathrm{i}}}{k_z^{\mathrm{i}}+n^2k_z^{\mathrm{t}}}, \tag{19c}$$

$$r^{\mathrm{p}}(k_x,k_y) = \frac{k_z^{\mathrm{i}}-n^2k_z^{\mathrm{t}}}{k_z^{\mathrm{i}}+n^2k_z^{\mathrm{t}}}, \tag{19d}$$

where we have defined $n$ as the relative index of refraction, $n = n_{\mathrm{i}}/n_{\mathrm{t}}$. We will concentrate on the reflection coefficients to calculate the reflected wave. The transmitted wave can be determined, but we will not show it explicitly as we can see later that this field does not give rise to an angular momentum transfer. The Taylor expansion of the reflection coefficients around $k_x = k_y = 0$, after applying the paraxial approximation, gives

$$r^{\mathrm{s}}(k_x) \approx \bar{r}^{\mathrm{s}} + \bar{r}'^{\mathrm{s}}k_x = \bar{r}^{\mathrm{s}}(1+\mathrm{i}k_xD^{\mathrm{s}}), \tag{20a}$$

$$r^{\mathrm{p}}(k_x) \approx \bar{r}^{\mathrm{p}} + \bar{r}'^{\mathrm{p}}k_x = \bar{r}^{\mathrm{p}}(1+\mathrm{i}k_xD^{\mathrm{p}}), \tag{20b}$$

where $\bar{r}^{\mathrm{s}}$ and $\bar{r}^{\mathrm{p}}$ are reflection coefficients evaluated at $k_x = k_y = 0$, and $\bar{r}'^{\mathrm{s}}$ and $\bar{r}'^{\mathrm{p}}$ are their derivatives with respect to $k_x$ at the same point in the reciprocal space. We define $\bar{r}'^{\mathrm{s}}/\bar{r}^{\mathrm{s}}$ and $\bar{r}'^{\mathrm{p}}/\bar{r}^{\mathrm{p}}$ to be $\mathrm{i}D^{\mathrm{s}}$ and $\mathrm{i}D^{\mathrm{p}}$ respectively and these correspond to longitudinal beam shifts [17, 18]. The dependence of reflection coefficients on $k_y$ is negligible as those terms including $k_y$ are much smaller than the mentioned terms.

With the given local incident plane wave $\mathbf{E}_{\mathrm{i}}(k_x,k_y)$, its local reflected plane wave can then be expressed as

$$\mathbf{E}_{\mathrm{r}}(k_x,k_y,t) = \left\{r^{\mathrm{s}}(k_x)E_{\mathrm{i}}^{\mathrm{s}}(\mathbf{k}_{\mathrm{i}})\mathbf{e}^{\mathrm{s}}(\mathbf{k}_{\mathrm{r}}) + r^{\mathrm{p}}(k_x)E_{\mathrm{i}}^{\mathrm{p}}(\mathbf{k}_{\mathrm{i}})\mathbf{e}^{\mathrm{p}}(\mathbf{k}_{\mathrm{r}})\right\} \times \mathrm{e}^{-\mathrm{i}\omega t+\mathrm{i}\mathbf{k}_{\mathrm{r}}\cdot\mathbf{r}}. \tag{21}$$

We note that $\mathbf{e}^{\mathrm{s}}(\mathbf{k}_{\mathrm{r}}) = \mathbf{e}^{\mathrm{s}}(\mathbf{k}_{\mathrm{i}})$ as they are normal to the same local plane of incidence, as depicted in figure 1. The reflected beam can then be determined directly to be

$$\mathbf{E}_{\mathrm{r}}(x,y,z,t) = \frac{1}{(2\pi)^2}\int_{-\infty}^{\infty}\int_{-\infty}^{\infty}\mathrm{d}k_x\mathrm{d}k_y\mathbf{E}_{\mathrm{r}}(k_x,k_y,t), \tag{22}$$

where the explicit form of $\mathbf{E}_{\mathrm{r}}(k_x,k_y,t)$ is

$$\begin{aligned}\mathbf{E}_{\mathrm{r}}(k_x,k_y,t) =& A_0\mathrm{e}^{-\mathrm{i}\omega t}\left\{\left(-\mathrm{i}r^{\mathrm{p}}\omega\alpha\cos\theta\right.\right.\\ &+\frac{\mathrm{i}r^{\mathrm{p}}c}{n}(\alpha k_x\sin\theta-\beta k_y\cot\theta\cos\theta)-\left.\frac{\mathrm{i}r^{\mathrm{s}}c\beta k_y}{n\sin\theta}\right)\mathbf{x}\\ &+\left(\mathrm{i}r^{\mathrm{s}}\omega\beta-\frac{\mathrm{i}c\alpha k_y\cot\theta}{n}(r^{\mathrm{s}}+r^{\mathrm{p}})\right)\mathbf{y}\\ &\left.-r^{\mathrm{p}}\left(\mathrm{i}\omega\alpha\sin\theta+\frac{\mathrm{i}c}{n}(\alpha k_x+\beta k_y)\cos\theta\right)\mathbf{z}\right\}\\ &\times\tilde{u}_l(k_x,k_y)\mathrm{e}^{\mathrm{i}\mathbf{k}_{\mathrm{r}}\cdot\mathbf{r}},\end{aligned} \tag{23}$$

where $\mathbf{k}_{\mathrm{r}} = (k_x\cos\theta+(k-\kappa)\sin\theta, k_y, -(k-\kappa)\cos\theta+k_x\sin\theta)$. The reflected beam $\mathbf{E}_{\mathrm{r}}(x,y,z,t)$ takes its simplest form when expressed in the reflection coordinates, and the coordinate transformation between the interface coordinates $(x,y,z)$ and the reflection coordinates $(x_{\mathrm{r}},y_{\mathrm{r}},z_{\mathrm{r}})$ is given by

$$\begin{aligned}x_{\mathrm{r}} &= -x\cos\theta - z\sin\theta,\\ y_{\mathrm{r}} &= y,\\ z_{\mathrm{r}} &= -z\cos\theta + x\sin\theta.\end{aligned} \tag{24}$$

Applying this transformation to Eq. 23 and substituting $\mathbf{E}_{\mathrm{r}}(k_x,k_y,t)$ into Eq. 22, the reflected electric and magnetic fields are

$$\mathbf{E}_{\mathrm{r}}(x_{\mathrm{r}},y_{\mathrm{r}},z_{\mathrm{r}},t) = A_0\left\{\chi_x\mathbf{x}_{\mathrm{r}}+\chi_y\mathbf{y}_{\mathrm{r}}+\chi_z\mathbf{z}_{\mathrm{r}}\right\}\mathrm{e}^{-\mathrm{i}\omega(t-nz_{\mathrm{r}}/c)}, \tag{25}$$

with

$$\chi_x = \mathrm{i}\omega\alpha\bar{r}^{\mathrm{p}}\left(\underline{u}_{k,l}-D^{\mathrm{p}}\frac{\partial\underline{u}_{k,l}}{\partial x_{\mathrm{r}}}\right)+\frac{c}{n}\beta\cot\theta(\bar{r}^{\mathrm{p}}+\bar{r}^{\mathrm{s}})\frac{\partial\underline{u}_{k,l}}{\partial y_{\mathrm{r}}}, \tag{26a}$$

$$\chi_y = \mathrm{i}\omega\beta\bar{r}^{\mathrm{s}}\left(\underline{u}_{k,l}-D^{\mathrm{s}}\frac{\partial\underline{u}_{k,l}}{\partial x_{\mathrm{r}}}\right)-\frac{c}{n}\alpha\cot\theta(\bar{r}^{\mathrm{p}}+\bar{r}^{\mathrm{s}})\frac{\partial\underline{u}_{k,l}}{\partial y_{\mathrm{r}}}, \tag{26b}$$

$$\chi_z = -\frac{c}{n}\left(\alpha\bar{r}^{\mathrm{p}}\frac{\partial\underline{u}_{k,l}}{\partial x_{\mathrm{r}}}+\beta\bar{r}^{\mathrm{s}}\frac{\partial\underline{u}_{k,l}}{\partial y_{\mathrm{r}}}\right), \tag{26c}$$

and

$$\begin{aligned}\mathbf{B}_{\mathrm{r}}(x_{\mathrm{r}},y_{\mathrm{r}},z_{\mathrm{r}},t) =& \frac{1}{\mathrm{i}\omega}\nabla\times\mathbf{E}_{\mathrm{r}}(x_{\mathrm{r}},y_{\mathrm{r}},z_{\mathrm{r}},t),\\ =& \frac{A_0}{c}\left\{n\chi_x\mathbf{y}_{\mathrm{r}}-n\chi_y\mathbf{x}_{\mathrm{r}}\right.\\ &\left.+c\left(\beta\bar{r}^{\mathrm{s}}\frac{\partial\underline{u}_{k,l}}{\partial x_{\mathrm{r}}}-\alpha\bar{r}^{\mathrm{p}}\frac{\partial\underline{u}_{k,l}}{\partial y_{\mathrm{r}}}\right)\mathbf{z}_{\mathrm{r}}\right\}\mathrm{e}^{-\mathrm{i}\omega(t-nz_{\mathrm{r}}/c)}.\end{aligned} \tag{27}$$

We have defined $\underline{u}_{k,l} = u_{k,l}(-x_{\mathrm{r}},y_{\mathrm{r}},z_{\mathrm{r}})$, where $u_{k,l}(x,y,z)$ is the complex function given in Eq. 2. These forms of the electric and magnetic fields respect the transverse property of free electromagnetic fields, as with the paraxial approximation $\nabla\cdot\mathbf{E}_{\mathrm{r}} = 0$ and $\nabla\cdot\mathbf{B}_{\mathrm{r}} = 0$. The minus sign in front of $x_{\mathrm{r}}$ indicates the change of the topological charge, from $l$ to $-l$, in the reflected beam.

The positive-frequency field operators corresponding to the classical fields, given in Eq. 8, Eq. 9, Eq. 25 and Eq. 27, in their own frames of reference according to the regular quantization procedure as in [19–21] are

$$\begin{aligned}\hat{\mathbf{E}}_{\mathrm{i}}^{+}(x_{\mathrm{i}},y_{\mathrm{i}},z_{\mathrm{i}},t) =& \int_0^{\infty}\mathrm{d}\omega\sqrt{\frac{\hbar}{4\pi\varepsilon_0cn\omega}}\hat{a}(\omega)\mathrm{e}^{-\mathrm{i}\omega(t-nz_{\mathrm{i}}/c)}\\ &\times\left\{\mathrm{i}\omega(\alpha\mathbf{x}_{\mathrm{i}}+\beta\mathbf{y}_{\mathrm{i}})u_{k,l}^{\mathrm{i}}\right.\\ &\left.-\frac{c}{n}\left(\alpha\frac{\partial u_{k,l}^{\mathrm{i}}}{\partial x_{\mathrm{i}}}+\beta\frac{\partial u_{k,l}^{\mathrm{i}}}{\partial y_{\mathrm{i}}}\right)\mathbf{z}_{\mathrm{i}}\right\},\end{aligned} \tag{28a}$$

$$\begin{aligned}\hat{\mathbf{B}}_{\mathrm{i}}^{+}(x_{\mathrm{i}},y_{\mathrm{i}},z_{\mathrm{i}},t) =& \int_0^{\infty}\mathrm{d}\omega\sqrt{\frac{\hbar}{4\pi\varepsilon_0c^3n\omega}}\hat{a}(\omega)\mathrm{e}^{-\mathrm{i}\omega(t-nz_{\mathrm{i}}/c)}\\ &\times\left\{-\mathrm{i}n\omega(\beta\mathbf{x}_{\mathrm{i}}-\alpha\mathbf{y}_{\mathrm{i}})u_{k,l}^{\mathrm{i}}\right.\\ &\left.+c\left(\beta\frac{\partial u_{k,l}^{\mathrm{i}}}{\partial x_{\mathrm{i}}}-\alpha\frac{\partial u_{k,l}^{\mathrm{i}}}{\partial y_{\mathrm{i}}}\right)\mathbf{z}_{\mathrm{i}}\right\},\end{aligned} \tag{28b}$$

$$\begin{aligned}\hat{\mathbf{E}}_{\mathrm{r}}^{+}(x_{\mathrm{r}},y_{\mathrm{r}},z_{\mathrm{r}},t) =& \int_0^{\infty}\mathrm{d}\omega\sqrt{\frac{\hbar}{4\pi\varepsilon_0cn\omega}}\hat{a}(\omega)\mathrm{e}^{-\mathrm{i}\omega(t-nz_{\mathrm{r}}/c)}\\ &\times\left\{\chi_x\mathbf{x}_{\mathrm{r}}+\chi_y\mathbf{y}_{\mathrm{r}}+\chi_z\mathbf{z}_{\mathrm{r}}\right\},\end{aligned} \tag{28c}$$

$$\begin{aligned}\hat{\mathbf{B}}_{\mathrm{r}}^{+}(x_{\mathrm{r}},y_{\mathrm{r}},z_{\mathrm{r}},t) =& \int_0^{\infty}\mathrm{d}\omega\sqrt{\frac{\hbar}{4\pi\varepsilon_0c^3n\omega}}\hat{a}(\omega)\mathrm{e}^{-\mathrm{i}\omega(t-nz_{\mathrm{r}}/c)}\\ &\times\left\{n\chi_x\mathbf{y}_{\mathrm{r}}-n\chi_y\mathbf{x}_{\mathrm{r}}\right.\\ &\left.+c\left(\beta\bar{r}^{\mathrm{s}}\frac{\partial\underline{u}_{k,l}}{\partial x_{\mathrm{r}}}-\alpha\bar{r}^{\mathrm{p}}\frac{\partial\underline{u}_{k,l}}{\partial y_{\mathrm{r}}}\right)\mathbf{z}_{\mathrm{r}}\right\},\end{aligned} \tag{28d}$$

where $u^{\mathrm{i}}_{k,l} \equiv u_{k,l}(x_{\mathrm{i}}, y_{\mathrm{i}}, z_{\mathrm{i}})$ and $\hat{a}(\omega)$ is the continuum photon annihilation operator which obeys the commutation relation:

$$\left[\hat{a}(\omega), \hat{a}^{\dagger}(\omega')\right] = \delta(\omega - \omega'). \tag{29}$$

As the field operators have the same space and time dependence as their classical versions, Maxwell's equations are manifestly satisfied. The normalization factors give the correct energy in a single-photon wave packet case. The single-photon pulse is represented by the state vector [20, 22],

$$|1\rangle = \int \mathrm{d}\omega \xi(\omega) \hat{a}^{\dagger}(\omega) |0\rangle , \tag{30}$$

where the state vector $|0\rangle$ represents the vacuum state. The function $\xi(\omega)$, which describes the distribution of probability amplitudes in the frequency domain, is normalized,

$$\int \mathrm{d}\omega \, |\xi(\omega)|^2 = 1. \tag{31}$$

It can conveniently be taken to be the narrowband Gaussian distribution function [13]

$$\xi(\omega) = \left(\frac{L^2}{2\pi c^2}\right)^{1/4} \exp\left[-\frac{L^2(\omega - \omega_0)^2}{4c^2}\right], \tag{32}$$

where $L$ is the spatial length of the pulse and $c/L \ll \omega_0$. This spectrum is centred at the central frequency $\omega_0$, and the spectral components of frequencies that are not in the range around the central frequency are very small.

One might think that to determine the reflected electric field we can treat the whole beam as an approximate plane wave with a wave vector $\mathbf{k}$ traveling in the direction of propagation to the interface and using the physics of reflection and transmission of plane waves to calculate the Fresnel coefficients directly so that the transmitted and reflected fields are given by the multiplication of those coefficients and the incident field, where the direction of propagation of the fields is given by geometrical optics. It is a good approximation, but this procedure leads to transmitted and reflected fields that are not transverse, in that $\nabla \cdot \mathbf{B}_{\mathrm{r}} \neq 0$, and therefore are unphysical and do not suffice for our purposes.

## 3. TOTAL FORCE AND TORQUE WITH PHYSICAL BOUNDARY CONDITIONS

With the dipole-based form, the force density acting on the dielectric at position $\mathbf{r}$ due to the light beam is [8, 9]

$$\mathbf{f}(\mathbf{r}, t) = (\mathbf{P}(\mathbf{r}, t) \cdot \nabla)\mathbf{E}(\mathbf{r}, t) + \frac{\partial \mathbf{P}(\mathbf{r}, t)}{\partial t} \times \mathbf{B}(\mathbf{r}, t). \tag{33}$$

As we focus on the interaction between light and the dielectric, there is no free charge and current included present.

The problem is that with the presence of the boundary the fields are not continuous and smooth, while the vector calculus is based on continuity and smoothness. Therefore, vector calculus identities should be cautiously applied. By writing Eq. 33 in terms of the electric displacement, $\mathbf{D} = \varepsilon_0 \mathbf{E} + \mathbf{P}$, and applying Maxwell's equations, Eq. 33 becomes

$$\begin{aligned}\mathbf{f} =& (\mathbf{D} \cdot \nabla)\mathbf{E} - \varepsilon_0 (\mathbf{E} \cdot \nabla)\mathbf{E} - \varepsilon_0 \mathbf{E} \times (\nabla \times \mathbf{E}) - \mathbf{B} \times (\nabla \times \mathbf{B}) \\ & - \varepsilon_0 \frac{\partial}{\partial t}(\mathbf{E} \times \mathbf{B}),\end{aligned} \tag{34}$$

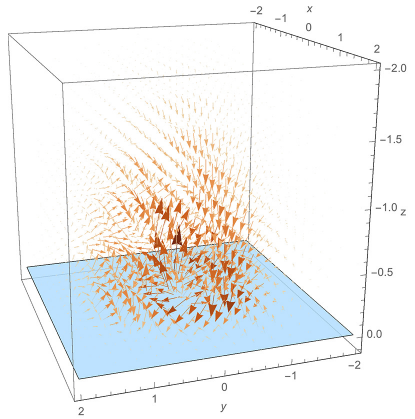


**Fig. 2.** The vector field of the force density acts on the dielectric medium inside it. The interface plane is located at $z = 0$ and the dielectric is occupied in the region $z < 0$. In the figure, we enhance the magnitude of the azimuthal force density, which is contained only in $\partial_t (\mathbf{P} \times \mathbf{B})$. This is the part that causes angular momentum transfer to the dielectric.

where the space and time dependence of the fields is omitted for brevity. The force density in Eq. 34 is depicted in figure 2. In this figure we present the intricate structure of the force density as the pulse hits the interface. We see that the azimuthal component circulates around the center of the beam. It is this that is responsible for the transfer of angular momentum to the dielectric.

In physics, we generally deal with discontinuity problems by introducing distribution functions, and a function with a jump can be expressed in terms of the Heaviside step function,

$$H(z) = \begin{cases} 0 & z < 0 \\ 1 & z > 0 \end{cases}, \tag{35}$$

We suppose that the interface is the $xy$-plane, or the plane $z = 0$ and the dielectric occupies the region $z < 0$. The $i$th component, where $i$ can take one of three values: $x$, $y$ and $z$, of the electric field is given by

$$E_i = E_i^{(\mathrm{in})} + (E_i^{(\mathrm{out})} - E_i^{(\mathrm{in})})H(z), \tag{36}$$

where $E_i^{(\mathrm{in})}$ and $E_i^{(\mathrm{out})}$ indicate the $i$th component of the electric field inside and outside the medium respectively. With the given definition of the step function, this equation apparently reflects the discontinuity of the electric field at the interface and the term on the left-hand side is now defined everywhere in space except the points lying at the interface. The other fields in Eq. 34, $\mathbf{D}$ and $\mathbf{B}$, are continuous but not smooth at the interface, so they need to be written in the same way as the electric field in Eq. 36.

The derivative of the step function gives the familiar Dirac delta function, and the product of these is half of the delta function, as from Eq. 35 only the part of the delta function in $z > 0$ survives,

$$\frac{\partial H(z)}{\partial z} = \delta(z), \tag{37a}$$

$$H(z)\delta(z) = \frac{\delta(z)}{2}. \tag{37b}$$

With every field being in the form of Eq. 36, using Eq. 37a and Eq. 37b and the fact that $1 - H(z) = H(-z)$, the $i$th component

of the force density is given by

$$
\begin{aligned}
f_i = &\left( D_z^{(\mathrm{in})}(E_z^{(\mathrm{out})} - E_z^{(\mathrm{in})}) - \varepsilon_0 \frac{((E_z^{(\mathrm{out})})^2 - (E_z^{(\mathrm{in})})^2)}{2} \right) \delta(z)\delta_{iz} \\
&+ \partial_l (D_l^{(\mathrm{in})} E_i^{(\mathrm{in})} + B_l^{(\mathrm{in})} B_i^{(\mathrm{in})}) H(-z) \\
&+ \partial_l (D_l^{(\mathrm{out})} E_i^{(\mathrm{out})} + B_l^{(\mathrm{out})} B_i^{(\mathrm{out})}) H(z) \\
&- \partial_i \left( \varepsilon_0 \frac{E_l^{(\mathrm{in})} E_l^{(\mathrm{in})}}{2} + \frac{B_l^{(\mathrm{in})} B_l^{(\mathrm{in})}}{2} \right) H(-z) \\
&- \partial_i \left( \varepsilon_0 \frac{E_l^{(\mathrm{out})} E_l^{(\mathrm{out})}}{2} + \frac{B_l^{(\mathrm{out})} B_l^{(\mathrm{out})}}{2} \right) H(z) \\
&- \partial_t (\varepsilon_0 \mathbf{E} \times \mathbf{B})_i, \qquad \textbf{(38)}
\end{aligned}
$$

where we defined $\partial_i$ as the derivative operators with respect to $x^i$ when $x^i \in \{x, y, z\}$ and $\delta_{ij}$ is the Kronecker delta. We have employed the summation convention with repeated indices, $l$, implying a summation over $x$ $y$ and $z$. To obtain the first and second terms of the equation we used the boundary condition that the electric field components parallel to the interface are continuous: $E_j^{(\mathrm{out})}\big|_{z=0^+} = E_j^{(\mathrm{in})}\big|_{z=0^-}$ where $j = x, y$, which means $(E_i^{(\mathrm{out})} - E_i^{(\mathrm{in})})\delta(z) = (E_z^{(\mathrm{out})} - E_z^{(\mathrm{in})})\delta(z)\delta_{iz}$.

Let us suppose that the observation is started at the time $t = -T$ and ended at $t = T$ and the center of the pulse is supposed to hit the interface approximately around $t = 0$. The time interval $2T$ is taken to be much larger than the time that the beam pulse take to pass the interface so that the period $2T$ includes the full interaction between the pulse and the interface. We can define the integration volume $V$ to be large in such a way that the photon pulse is inside it during the observation and there is no field at the surface of $V$. This automatically implies that the terms being in the form of the derivatives with respect to $x$ and $y$ in Eq. 38 will not contribute to the total force after integration over the volume $V$. The terms with the $z$ derivative, on the other hand, will exactly cancel with the first two terms that contain the delta function after the integration using the physical boundary conditions, when there is no free charge and current,

$$
E_j^{(\mathrm{out})}\Big|_{z=0^+} = E_j^{(\mathrm{in})}\Big|_{z=0^-}; \qquad j = x, y, \qquad \textbf{(39a)}
$$

$$
\mathbf{B}^{(\mathrm{out})}\Big|_{z=0^+} = \mathbf{B}^{(\mathrm{in})}\Big|_{z=0^-}, \qquad \textbf{(39b)}
$$

$$
D_z^{(\mathrm{out})}\Big|_{z=0^+} = D_z^{(\mathrm{in})}\Big|_{z=0^-}. \qquad \textbf{(39c)}
$$

Therefore, only the last term in Eq. 38 remains:

$$
\int_V \mathbf{f} \mathrm{d}V = -\int_V \mathrm{d}V \partial_t (\varepsilon_0 \mathbf{E} \times \mathbf{B}) = -\partial_t \int_V \mathrm{d}V (\varepsilon_0 \mathbf{E} \times \mathbf{B}). \qquad \textbf{(40)}
$$

This equation is a manifestation of Newton's third law, with the kinetic momentum of light being in the Abraham form: $c^{-2}(\mathbf{E} \times \mathbf{H})$ [10, 11, 23]. The force that the photon exerts on the dielectric is of the same magnitude as the force that the dielectric gives to the photon but in the opposite direction. We now see that once the physical boundary conditions are applied, the Lorentz force reproduces Newton's third law of motion straightforwardly. With the form of Eq. 40 in the case of total internal reflection with a glass-air interface, we see that the evanescent field can contribute some force to the dielectric, while this interpretation cannot be directly realized in the form of the dipole-based force density as there is no polarization outside the dielectric, which directly implies no force density outside the medium. However, because the evanescent field outside the medium is not long-lasting, its effects cancel as time evolves and hence it provides no net contribution. As Eq. 40 agrees with the third law of motion, the conservation of linear momentum is satisfied.

From Eq. 38 and the chain rule, the torque density is directly given by

$$
\tau_i = \epsilon_{ijk} x_j f_k \qquad \textbf{(41)}
$$

where $\epsilon_{ijk}$ is the Levi-Civita symbol and $f_k$ is the force density given in Eq. 38. We used the fact that the electric field $\mathbf{E}$ and the electric displacement $\mathbf{D}$ are parallel to each other in linear, homogeneous and isotropic lossless media, where the refractive indices are real numbers. The vector product of these two fields then vanishes: $\mathbf{D} \times \mathbf{E} = \mathbf{0}$. Integration over space, in the same manner as for the force density case, gives the total torque:

$$
\boldsymbol{\mathcal{T}} = \int_V \boldsymbol{\tau} \mathrm{d}V = -\partial_t \int_V \mathrm{d}V (\mathbf{r} \times (\varepsilon_0 \mathbf{E} \times \mathbf{B})). \qquad \textbf{(42)}
$$

This equation clearly guarantees the conservation of the total mechanical or kinetic angular momentum. The evanescent field also makes a torque at an instant time around $t = 0$, but this torque again cancels itself as time evolves.

## 4. EFFECTIVE TORQUE AND ANGULAR MOMENTUM TRANSFER

This section is devoted to determining the enacted torque on the dielectric by the photon pulse and the associated angular momentum transfer. The total force and linear momentum can also be calculated by using Eq. 40 and the electric and magnetic operators given in section 2. This work, however, focuses mainly on torque and angular momentum. From Eq. 42, the expectation of the total torque exerted on the dielectric due to total internal reflection of a single-photon pulse is given by

$$
< \boldsymbol{\mathcal{T}} > = -\varepsilon_0 \frac{\partial}{\partial t} \int_V \mathrm{d}V \left( \mathbf{r} \times \left( \langle 1| : \hat{\mathbf{E}}^- \times \hat{\mathbf{B}}^+ + \hat{\mathbf{E}}^+ \times \hat{\mathbf{B}}^- : |1\rangle \right) \right), \qquad \textbf{(43)}
$$

where

$$
\hat{\mathbf{E}}^- \times \hat{\mathbf{B}}^+ = \left( \hat{\mathbf{E}}_{\mathrm{i}}^- + \hat{\mathbf{E}}_{\mathrm{r}}^- \right) \times \left( \hat{\mathbf{B}}_{\mathrm{i}}^+ + \hat{\mathbf{B}}_{\mathrm{r}}^+ \right) H(-z) + \left( \hat{\mathbf{E}}_{\mathrm{t}}^- \times \hat{\mathbf{B}}_{\mathrm{t}}^+ \right) H(z). \qquad \textbf{(44)}
$$

The subscripts i, r and t are used to denote the incident, reflected and transmitted fields respectively. The terms in $\mathbf{E} \times \mathbf{B}$ containing two annihilation and creation operators are omitted as they do not contribute to the expectation value for the single photon state. We use the colons to notify that the operators between these two colons are in normal order [24]. Even though there are numerous terms involved in Eq. 43 and Eq. 44, only some of these give effective torques, the ones that do not cancel themselves when time evolves. As mentioned, the evanescent field exists only when the pulse hits the interface, only within a short period of time. The torque caused by this field is not effective, and the same goes for the cross terms:

$$
\begin{aligned}
< \boldsymbol{\mathcal{T}}^{\mathrm{ineff}} > = -\frac{\partial}{\partial t} \int_V \mathrm{d}V \mathbf{r} \times (\langle 1| : (\hat{\mathbf{p}}_{\mathrm{ir}} + \hat{\mathbf{p}}_{\mathrm{ri}}) H(-z) \\
+ \hat{\mathbf{p}}_{\mathrm{tt}} H(z) : |1\rangle), \qquad \textbf{(45)}
\end{aligned}
$$

where the vector product between the electric field of the beam $i$ and the magnetic field of the beam $j$ is denoted by

$$
\hat{\mathbf{p}}_{ij} \equiv \varepsilon_0 \hat{\mathbf{E}}_i^- \times \hat{\mathbf{B}}_j^+ + \mathrm{h.c.}, \qquad \textbf{(46)}
$$

and h.c. denotes the Hermitian conjugate of the preceding terms. Only the effective torques can cause angular momentum transfer because they are still valid after integration over the observation time, and we will focus only on these:

$$\begin{aligned} <\boldsymbol{\mathcal{T}}^{\text{eff}}> &= -\frac{\partial}{\partial t}\int_V \mathrm{d}V\left(\mathbf{r}\times\left(\langle 1|:\hat{\mathbf{p}}_{\text{ii}}+\hat{\mathbf{p}}_{\text{rr}}:|1\rangle\right)\right)H(-z) \\ &= <\boldsymbol{\mathcal{T}}^{\text{eff}}_{\text{i}}> + <\boldsymbol{\mathcal{T}}^{\text{eff}}_{\text{r}}>, \end{aligned} \tag{47}$$

where

$$<\boldsymbol{\mathcal{T}}^{\text{eff}}_{\text{i(r)}}> = -\frac{\partial}{\partial t}\int_V \mathrm{d}V\left(\mathbf{r}\times\left(\langle 1|:\hat{\mathbf{p}}_{\text{ii(rr)}}:|1\rangle\right)\right)H(-z). \tag{48}$$

Recall that the electric and magnetic fields of the incident and reflected fields will be in the simplest forms when they are written in terms of their own coordinates. The benefit of writing the effective torque in the form of the second line of Eq. 47 is that we can calculate the torques caused by incident and reflected beams in their own coordinates separately, because torques are vectors, and rotations of coordinate systems are passive transformation for vectors (or more precisely pseudovectors). Only their descriptions are changed. In other words, the electric and magnetic field operators given in Eqs. 28 can be directly used. Once we have evaluated these torques, $<\boldsymbol{\mathcal{T}}^{\text{eff}}_{\text{i}}>$ and $<\boldsymbol{\mathcal{T}}^{\text{eff}}_{\text{r}}>$ written in terms of their own coordinates, the incident and reflected coordinates respectively, one can then use the previously given rotational transformations, Eq. 10 and Eq. 24, to express these torques in terms of the interface coordinates. With the given rotational transformations, the step function $H(-z)$ in the incident and reflected coordinates is directly given by

$$H(-z) = H(x_{\text{i}}\tan\theta - z_{\text{i}}) = H(z_{\text{r}} + x_{\text{r}}\tan\theta). \tag{49}$$

The effective torque given by the incident beams is then

$$\begin{aligned} <\boldsymbol{\mathcal{T}}^{\text{eff}}_{\text{i}}> = &-\frac{\partial}{\partial t}\int_{-\infty}^{\infty}\int_{-\infty}^{\infty}\mathrm{d}x_{\text{i}}\mathrm{d}y_{\text{i}}\int_{-\infty}^{0}\mathrm{d}z_{\text{i}}\mathbf{r}\times\left(\langle 1|:\hat{\mathbf{p}}_{\text{ii}}:|1\rangle\right) \\ &-\frac{\partial}{\partial t}\int_{-\infty}^{\infty}\int_{-\infty}^{\infty}\mathrm{d}x_{\text{i}}\mathrm{d}y_{\text{i}}\int_{0}^{x_{\text{i}}\tan\theta}dz_{\text{i}}\left(\mathbf{r}\times\langle 1|:\hat{\mathbf{p}}_{\text{ii}}:|1\rangle\right) \end{aligned} \tag{50}$$

The integration over the observation time of the last term vanishes, so it makes no net angular momentum transfer. This can be verified easily as at both start and stop times there is no incident field in the region between $z_{\text{i}} = 0$ and $z_{\text{i}} = x_{\text{i}}\tan\theta$. The same holds for the torque from the reflected part,

$$<\boldsymbol{\mathcal{T}}^{\text{eff}}_{\text{r}}> = -\frac{\partial}{\partial t}\int_{-\infty}^{\infty}\int_{-\infty}^{\infty}\mathrm{d}x_{\text{r}}\mathrm{d}y_{\text{r}}\int_{0}^{\infty}\mathrm{d}z_{\text{r}}\left(\mathbf{r}\times\langle 1|:\hat{\mathbf{p}}_{\text{rr}}:|1\rangle\right). \tag{51}$$

We assume that the refractive index of the medium does not vary much with the wave frequency: $n(\omega') \approx n(\omega) = n$. Using Eqs. 28, the normal ordered Poynting vector operator of the incident beam may be written as

$$\begin{aligned} (\varepsilon_0 c^2)^{-1}\hat{\mathbf{S}}_{\text{i}} &= :\hat{\mathbf{E}}^{-}_{\text{i}}\times\hat{\mathbf{B}}^{+}_{\text{i}} + \hat{\mathbf{E}}^{+}_{\text{i}}\times\hat{\mathbf{B}}^{-}_{\text{i}}: \\ &= \frac{\hbar}{4\pi\varepsilon_0 c^2 n}\int_0^\infty\int_0^\infty \mathrm{d}\omega\mathrm{d}\omega'\frac{1}{\sqrt{\omega\omega'}}\hat{a}^\dagger(\omega)\hat{a}(\omega') \\ &\quad\times \mathrm{e}^{\mathrm{i}(\omega-\omega')(t-nz_{\text{i}}/c)}\left\{\mathcal{S}^x_{\text{i}}\mathbf{x}_{\text{i}} + \mathcal{S}^y_{\text{i}}\mathbf{y}_{\text{i}} + \mathcal{S}^z_{\text{i}}\mathbf{z}_{\text{i}}\right\}, \end{aligned} \tag{52}$$

with

$$\begin{aligned} \mathcal{S}^x_{\text{i}} =& -\mathrm{i}\omega c(u^{\text{i}}_{k,l})^*\partial_{x_{\text{i}}}u^{\text{i}}_{k',l} + \mathrm{i}\omega' c u^{\text{i}}_{k',l}\partial_{x_{\text{i}}}(u^{\text{i}}_{k,l})^* \\ &+ c\sigma_{\text{i}}\left(\omega(u^{\text{i}}_{k,l})^*\partial_{y_{\text{i}}}u^{\text{i}}_{k',l} + \omega' u^{\text{i}}_{k',l}\partial_{y_{\text{i}}}(u^{\text{i}}_{k,l})^*\right), \end{aligned} \tag{53a}$$

$$\begin{aligned} \mathcal{S}^y_{\text{i}} =& -\mathrm{i}\omega c(u^{\text{i}}_{k,l})^*\partial_{y_{\text{i}}}u^{\text{i}}_{k',l} + \mathrm{i}\omega' c u^{\text{i}}_{k',l}\partial_{y_{\text{i}}}(u^{\text{i}}_{k,l})^* \\ &- c\sigma_{\text{i}}\left(\omega(u^{\text{i}}_{k,l})^*\partial_{x_{\text{i}}}u^{\text{i}}_{k',l} + \omega' u^{\text{i}}_{k',l}\partial_{x_{\text{i}}}(u^{\text{i}}_{k,l})^*\right), \end{aligned} \tag{53b}$$

$$\mathcal{S}^z_{\text{i}} = 2n\omega\omega'(u^{\text{i}}_{k,l})^* u^{\text{i}}_{k',l}, \tag{53c}$$

where $\sigma_{\text{i}} = \mathrm{i}(\alpha\beta^* - \alpha^*\beta)$ is the spin angular momentum quantum number of the incident beam. To obtain the expectation value of the Poynting vector in Eq. 52 one can replace annihilation and creation operators with the function $\xi(\omega')$ and its complex conjugate $\xi^*(\omega)$. With the narrowband wave packet state of the single-photon pulse defined previously, the frequencies $\omega$ and $\omega'$ in the integrand can then be approximately replaced with the central frequency $\omega_0$, with the exception of the difference: $\omega - \omega'$. Substituting back to Eq. 50, the expectation of the torque from the incident part then becomes

$$\begin{aligned} <\boldsymbol{\mathcal{T}}^{\text{eff}}_{\text{i}}> =& -\frac{\hbar}{2\pi cn}(l+\sigma_{\text{i}})\mathbf{z}_{\text{i}}\int_{-\infty}^{0}\mathrm{d}z_{\text{i}}\int_0^\infty\int_0^\infty \mathrm{d}\omega\mathrm{d}\omega'\xi^*(\omega)\xi(\omega') \\ &\times \mathrm{i}(\omega-\omega')\mathrm{e}^{\mathrm{i}(\omega-\omega')(t-nz_{\text{i}}/c)} \\ =& \frac{\hbar}{n^2}\sqrt{\frac{2c^2}{\pi L^2}}(l+\sigma_{\text{i}})\mathbf{z}_{\text{i}}\mathrm{e}^{-2t^2c^2/L^2}. \end{aligned} \tag{54}$$

The angular momentum transfer due to this part of the effective torque is simply

$$\lim_{T\to\infty}\int_{-T}^{T}\mathrm{d}t <\boldsymbol{\mathcal{T}}^{\text{eff}}_{\text{i}}> = \frac{\hbar}{n^2}(l+\sigma_{\text{i}})\mathbf{z}_{\text{i}}. \tag{55}$$

The components in $\mathbf{x}_{\text{i}}$ and $\mathbf{y}_{\text{i}}$ directions do not appear because, after applying the narrow-bandwidth approximation, the term $\mathcal{S}^z_{\text{i}}$ is symmetric about both $x_{\text{i}}$ and $y_{\text{i}}$ axes, and integrations of odd functions vanish.

As the forms of the reflected fields are more complicated than those of the incident fields, the effective torque given by these fields contains many terms. However, with the help of the symmetry in the $x_{\text{r}}y_{\text{r}}$-plane of the strength of the complex function $\left|\underline{u}_{k,l}\right|^2$ some of these can then be omitted as their integrations vanish. The expectation value of the effective torque caused by the reflected part is then written as

$$\begin{aligned} <\boldsymbol{\mathcal{T}}^{\text{eff}}_{\text{r}}> =& -\frac{\hbar}{4\pi c^2 n}\frac{\partial}{\partial t}\int_0^\infty \mathrm{d}z_{\text{r}}\left(\int_0^\infty\int_0^\infty \mathrm{d}\omega\mathrm{d}\omega'\xi^*(\omega)\xi(\omega')\right. \\ &\times \mathrm{e}^{\mathrm{i}(\omega-\omega')(t-nz_{\text{r}}/c)} \\ &\left.\times\int_{-\infty}^{\infty}\int_{-\infty}^{\infty}\mathrm{d}x_{\text{r}}\mathrm{d}y_{\text{r}}\left\{\mathcal{J}^x_{\text{r}}\mathbf{x}_{\text{r}} + \mathcal{J}^y_{\text{r}}\mathbf{y}_{\text{r}} + \mathcal{J}^z_{\text{r}}\mathbf{z}_{\text{r}}\right\}\right), \end{aligned} \tag{56}$$

with

$$\mathcal{J}^x_{\text{r}} = 2c(\sigma_{\text{i}} + \sigma_{\text{r}})y_{\text{r}}\cot\theta\partial_{y_{\text{r}}}\left|\underline{u}_{k_0,l}\right|^2, \tag{57a}$$

$$\mathcal{J}^y_{\text{r}} = 2\omega_0 n\left(|\alpha|^2 D^{\text{p}} + |\beta|^2 D^{\text{s}}\right)x_{\text{r}}\partial_{x_{\text{r}}}\left|\underline{u}_{k_0,l}\right|^2 \tag{57b}$$

$$\begin{aligned} \mathcal{J}^z_{\text{r}} =& \mathrm{i}cx_{\text{r}}(\underline{u}_{k_0,l}\partial_{y_{\text{r}}}\underline{u}^*_{k_0,l} - \underline{u}^*_{k_0,l}\partial_{y_{\text{r}}}\underline{u}_{k_0,l}) - c\sigma_{\text{r}}x_{\text{r}}\partial_{x_{\text{r}}}\left|\underline{u}_{k_0,l}\right|^2 \\ &- \mathrm{i}cy_{\text{r}}(\underline{u}_{k_0,l}\partial_{x_{\text{r}}}\underline{u}^*_{k_0,l} - \underline{u}^*_{k_0,l}\partial_{x_{\text{r}}}\underline{u}_{k_0,l}) + c\sigma_{\text{r}}x_{\text{r}}\partial_{x_{\text{r}}}\left|\underline{u}_{k_0,l}\right|^2, \end{aligned} \tag{57c}$$

where we defined $\alpha' = \bar{r}^{\rm p}\alpha$ and $\beta' = \bar{r}^{\rm s}\beta$ which can be thought of as approximate polarizations of the reflected beam. We also defined $\sigma_{\rm r} = {\rm i}(\alpha'\beta'^{*} - \alpha'^{*}\beta')$ to be the spin quantum number of the reflected beam. The terms whose integration over the $x_{\rm r}y_{\rm r}$-plane vanish are not shown explicitly in the above equations. With symmetry and relabeling, the effective torque from the reflected fields may be written in the form

$$< \boldsymbol{\mathcal{T}}^{\rm eff}_{\rm r} >= \frac{\hbar}{n^2}\sqrt{\frac{2c^2}{\pi L^2}}\,{\rm e}^{-2t^2c^2/L^2}\left\{(\sigma_{\rm i}+\sigma_{\rm r})\cot\theta\mathbf{x}_{\rm r} + (l-\sigma_{\rm r})\mathbf{z}_{\rm r} + \frac{\omega_0 n}{c}(|\alpha|^2 D^{\rm p} + |\beta|^2 D^{\rm s})\mathbf{y}_{\rm r}\right\}. \quad \textbf{(58)}$$

The effective torques in the $x_{\rm r}$ and $y_{\rm r}$ directions actually appear because the reflected beam is shifted in both longitudinal and transverse directions. This can be verified by determining the center of gravity of the reflected beam and by the corresponding torque. We note that this torque is associated with a change in the mechanical, or Abraham, angular momentum of the photon. The Minkowski angular momentum, by contrast, is unchanged [25, 26] and, indeed, its constancy has been used to obtain the form of the beam shift in analogy to the Hall effect [27, 28].

By expressing the effective torques $< \boldsymbol{\mathcal{T}}^{\rm eff}_{\rm i} >$ and $< \boldsymbol{\mathcal{T}}^{\rm eff}_{\rm r} >$ in terms of the interface coordinates $(x, y, z)$, the total effective torque is then given by

$$\begin{aligned} < \boldsymbol{\mathcal{T}}^{\rm eff} >&= < \boldsymbol{\mathcal{T}}^{\rm eff}_{\rm i} > + < \boldsymbol{\mathcal{T}}^{\rm eff}_{\rm r} > \\ &= \frac{\hbar}{n^2}\sqrt{\frac{2c^2}{\pi L^2}}\,{\rm e}^{-2t^2c^2/L^2}\left\{-(\sigma_{\rm i}+\sigma_{\rm r})\cos\theta\mathbf{z} - (\sigma_{\rm i}+\sigma_{\rm r})\cot\theta\cos\theta\mathbf{x} + \frac{\omega_0 n}{c}(|\alpha|^2 D^{\rm p} + |\beta|^2 D^{\rm s})\mathbf{y}\right. \\ &\quad \left.\left[(2l+(\sigma_{\rm i}-\sigma_{\rm r}))\sin\theta\mathbf{x} + (\sigma_{\rm i}+\sigma_{\rm r})\cos\theta\mathbf{z}\right]\right\}. \quad \textbf{(59)} \end{aligned}$$

The exponential term indicates that the photon exerts a torque on the dielectric only when it hits the interface, and there is no net torque appearing elsewhere while it is traveling inside the dielectric. The part of the effective torque corresponding to the transfer of the intrinsic angular momentum of the photon to the dielectric is separated from the rest of the effective torque, given by the beam shift effect, by the square bracket in the last line of Eq. 59.

## 5. DOVE PRISM APPLICATION

This section evaluates the angular momentum transfer to an M-shaped Dove prism, as depicted in figure 3. This type of Dove prism is generally designed to convert the polarization state of photons in the same manner as a quarter-wave plate [29], and also inverts the orbital angular momentum of incoming photons like other Dove prisms. Our aim is to account for the observed change in the intrinsic angular momentum of the light [30], $-\hbar(2l+\sigma_{\rm in}-\sigma_{\rm out})\mathbf{x}_0$, where $(\sigma_{\rm in}-\sigma_{\rm out})$ denotes the change in polarization of the light. For this reason, we concentrate here on the contribution in the square bracket in Eq. 59. The remaining parts account for for a small torque associated with the shift of the beam center in the plane perpendicular to the propagation axis:

$$< \boldsymbol{\mathcal{T}}^{\rm eff}_{\rm intrinsic} >= \frac{\hbar}{n^2}\sqrt{\frac{2c^2}{\pi L^2}}\,{\rm e}^{-2t^2c^2/L^2}\left[(2l+(\sigma_{\rm i}-\sigma_{\rm r}))\sin\theta\mathbf{x} + (\sigma_{\rm i}+\sigma_{\rm r})\cos\theta\mathbf{z}\right]. \quad \textbf{(60)}$$

The angular momentum change of the dielectric arising from this torque is

$$\begin{aligned} < \Delta\mathbf{L}_{\rm dielectric} >&= \int_{-\infty}^{\infty} {\rm d}t < \boldsymbol{\mathcal{T}}^{\rm eff}_{\rm intrinsic} > \\ &= \frac{\hbar}{n^2}((2l+(\sigma_{\rm i}-\sigma_{\rm r}))\sin\theta\mathbf{x} + (\sigma_{\rm i}+\sigma_{\rm r})\cos\theta\mathbf{z}). \end{aligned} \quad \textbf{(61)}$$

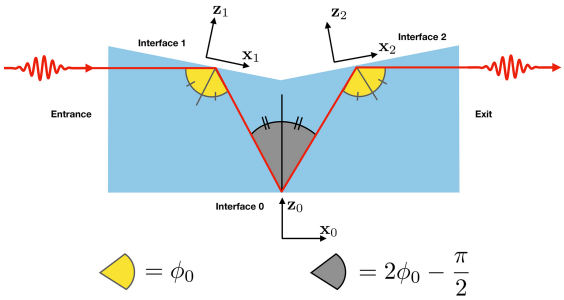


**Fig. 3.** The figure illustrates the optical path of the single-photon pulse passing through the M-shaped Dove prism.

With the geometric configuration of the Dove prism shown in figure 3, there are three total internal reflections involved. Following Loudon, [13], we note that there are five different positions at which the angular momentum of the photon is changed and transferred to the dielectric: these are the points where the photon hits the interfaces. To calculate the angular momentum transfer due to three total internal reflection processes, we introduce three different coordinate systems, as shown in the figure. The rotational transformations of the unit vectors between those coordinates are given by

$$\mathbf{x}_1 = \mathbf{x}_0\sin\phi_0 - \mathbf{z}_0\cos\phi_0, \quad \textbf{(62a)}$$
$$\mathbf{z}_1 = \mathbf{z}_0\sin\phi_0 + \mathbf{x}_0\cos\phi_0, \quad \textbf{(62b)}$$
$$\mathbf{x}_2 = \mathbf{x}_0\sin\phi_0 + \mathbf{z}_0\cos\phi_0, \quad \textbf{(62c)}$$
$$\mathbf{z}_2 = \mathbf{z}_0\sin\phi_0 - \mathbf{x}_0\cos\phi_0. \quad \textbf{(62d)}$$

We suppose that the incident single photon initially has spin angular momentum $\hbar\sigma_{\rm in}$ and orbital angular momentum $\hbar l$ in the positive $x_0$ direction. The direction of polarization of a single photon is not changed if it passes normally through a dielectric interface. The spin angular-momentum quantum number is conserved after the single photon entering the entrance surface. With this transformation, the total change of angular momentum of the Dove prism due to three total internal reflections is given by

$$\begin{aligned} < \Delta\mathbf{L}_{\rm total} >&= < \Delta\mathbf{L}_1 > + < \Delta\mathbf{L}_0 > + < \Delta\mathbf{L}_2 > \\ &= \frac{\hbar}{n^2}\{(2l+(\sigma_{\rm in}-\sigma_1))\sin\phi_0\mathbf{x}_1 \\ &\quad +(\sigma_{\rm in}+\sigma_1)\cos\phi_0\mathbf{z}_1 \\ &\quad +(-2l+(\sigma_1-\sigma_2))\sin(2\phi_0-\pi/2)\mathbf{x}_0 \\ &\quad -(\sigma_1+\sigma_2)\cos(2\phi_0-\pi/2)\mathbf{z}_0 \\ &\quad +(2l+(\sigma_2-\sigma_{\rm out}))\sin\phi_0\mathbf{x}_2 \\ &\quad +(\sigma_2+\sigma_{\rm out})\cos\phi_0\mathbf{z}_2\} \\ &= \frac{\hbar}{n^2}(2l+(\sigma_{\rm in}-\sigma_{\rm out}))\mathbf{x}_0, \end{aligned} \quad \textbf{(63)}$$

where $\sigma_1$ and $\sigma_2$ are the spin angular-momentum quantum numbers of the beam after encountering first and second total internal reflections, and $\sigma_{\text{out}}$ is the spin quantum number of the outgoing photon. We used $< \Delta \mathbf{L}_j >$ to represent the angular momentum change after the photon hit the interface $j$. Each time that the beam is reflected the topological charge is flipped from $l$ to $-l$ or vice versa. From [13], we know that the angular momentum transfer at the entrance and the exit points are

$$< \Delta \mathbf{L}_{\text{entrance}} >= \hbar(l_{\text{in}} + \sigma_{\text{in}}) \left(1 - \frac{1}{n^2}\right) \mathbf{x}_0, \tag{64a}$$

$$< \Delta \mathbf{L}_{\text{exit}} >= -\hbar(l_{\text{out}} + \sigma_{\text{out}}) \left(1 - \frac{1}{n^2}\right) \mathbf{x}_0. \tag{64b}$$

where $l_{\text{in}}$ ($l_{\text{out}}$) is the topological charge the incoming (outgoing) beam. As we supposed that the incoming photon has an orbital angular momentum $\hbar l_{\text{in}} = \hbar l$ and the Dove prism inverts the orbital angular momentum of the outgoing beam, the outgoing photon at the exit point will have the orbital angular momentum $\hbar l_{\text{out}} = -\hbar l$. Combining this result with the one we obtained in Eq. 63, we find that in the case that the single photon pulse passes through the Dove prism, the angular momentum change of the Dove prism is

$$\begin{aligned} < \Delta \mathbf{L}_{\text{Dove}} >= & \hbar(l + \sigma_{\text{in}}) \left(1 - \frac{1}{n^2}\right) \mathbf{x}_0 + \frac{\hbar}{n^2}(2l + (\sigma_{\text{in}} - \sigma_{\text{out}}))\mathbf{x}_0 \\ & - \hbar(-l + \sigma_{\text{out}}) \left(1 - \frac{1}{n^2}\right) \mathbf{x}_0, \\ = & \hbar(2l + (\sigma_{\text{in}} - \sigma_{\text{out}}))\mathbf{x}_0. \end{aligned} \tag{65}$$

As this M-shaped Dove prism manipulates polarization in the same way as a quarter-wave plate, if the incoming photon is circularly polarized, $\sigma_{\text{in}} = 1$, the outgoing will be linearly polarized, $\sigma_{\text{out}} = 0$. The angular momentum change of the Dove prism due to the intrinsic angular momentum transfer from a single-photon pulse in this case is then

$$< \Delta \mathbf{L}_{\text{Dove}} >= (2l + 1)\hbar \mathbf{x}_0, \tag{66}$$

in the direction of propagation of the outgoing photon, while the angular momentum of the photon itself is changed by $< \Delta \mathbf{L}_{\text{photon}} >= -(2l + 1)\hbar \mathbf{x}_0$. Clearly, the total angular momentum is conserved as required. The change of angular momentum of the Dove prism and the torques exerted on it at each interface are shown in figure 4 for the case of an incident photon with topological charge $l = 1$ and spin quantum number $\sigma_{\text{in}} = 1$, while the longitudinal force and momentum transfer are depicted in figure 5. We note that there is an asymmetry in the torque that is not apparent in the longitudinal force. The origin of this is the change in the polarization of the light on reflection which affects the angular momentum but not the linear momentum.

## 6. CONCLUSION

We have demonstrated that the angular spectrum method can be employed to determine transverse reflected fields. The physical boundary conditions lead us to results fully in accord with Newton's third law: the force that photons exert on a dielectric is equal and opposite to that which the dielectric exerts on the photons. The third law ensures the conservation of both linear and angular momentum. We discussed the torque exerted on the dielectric via total internal reflection. The result shows that photons only exert a net torque on the dielectric when they hit the interface. The shifting effect also produces an effective torque on the dielectric, but this torque does not correspond to a net change of intrinsic angular momentum of photons. We applied our results to analyze the angular momentum transfer to the M-shaped Dove prism and found an angular momentum transfer fully consistent with the observed change in angular momentum of the light.

Finally, we expect similar torques to exist in other optical components that transform the angular momentum of light. These include, in particular, astigmatic mode converters [31], which have been shown to transform the orbital angular momentum as the light propagates through the lenses [32].

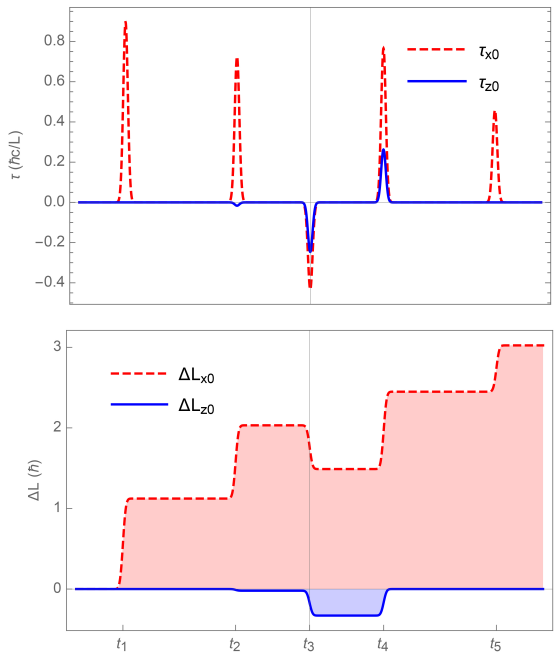


**Fig. 4.** The effective torques given by the light pulse with orbital angular momentum $\hbar$ and the angular momentum change of the Dove prism when the photon hitting each interface at the time $t_1$, $t_2$, $t_3$, $t_4$ and $t_5$ consequently. The red dashed line and the blue solid line represent the torques and angular momentum change in $\mathbf{x}_0$ and $\mathbf{z}_0$ directions respectively.

## FUNDING

Development and Promotion of Science and Technology Talents Project (DPST), Thailand; Royal Society (RP150122).

## ACKNOWLEDGMENTS

We would like to thank Jörg B Götte for helpful discussions.

## REFERENCES

1. J. H. Poynting, "The wave motion of a revolving shaft, and a suggestion as to the angular momentum in a beam of circularly polarised light," Proc. Roy. Soc. A **82** 560 (1909).
2. L. Allen, M. W. Beijersbergen, R. J. C. Spreeuw, and J. P. Woerdman, "Orbital angular momentum of light and the transformation of Laguerre-Gaussian laser modes," Phys. Rev. A **45** 8185 (1992).
3. S. J. van Enk and G. Nienhuis, "Commutation rules and eigenvalues of spin and orbital angular momentum of radiation fields," J. Mod. Opt. **41** 963 (1994).

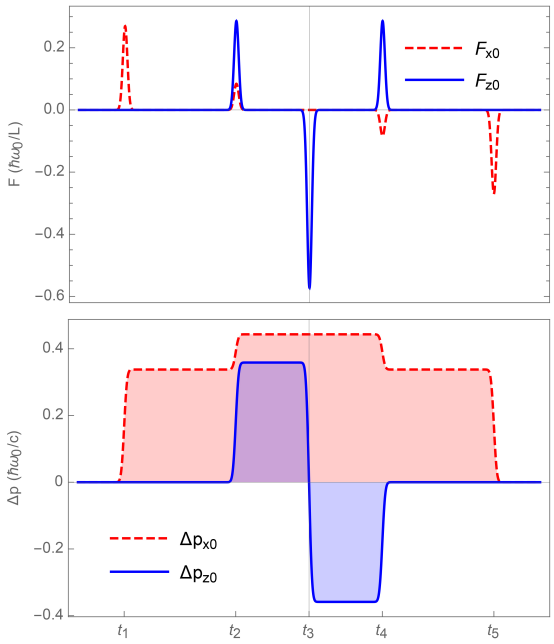


**Fig. 5.** The longitudinal force acting on the Dove prism when the photon hitting each of its interfaces at the time $t_1$, $t_2$, $t_3$, $t_4$ and $t_5$ consequently, and its momentum change due to the force.


4. S. J. van Enk and G. Nienhuis, "Spin and orbital angular momentum of photons," EPL **25** 497 (1994).
5. S. M. Barnett, "Rotation of electromagnetic fields and the nature of optical angular momentum," J. Mod. Opt. **57** 1339 (2010).
6. S. M. Barnett, L. Allen, R. P. Cameron, C. R. Gilson, M. J. Padgett, F. C. Speirits, and A. M. Yao, "On the natures of the spin and orbital parts of optical angular momentum," J. Opt. **18** 064004 (2016).
7. E. Noether, "Invariante Variationsprobleme," Kgl. Ges. d. Wiss. Nachrichten, Math.-phys. Klasse. 235 (1918).
8. J. P. Gordon, "Radiation forces and momenta in dielectric media," Phys. Rev. A. **8** 14 (1973).
9. S. M. Barnett and R. Loudon, "On the electromagnetic force on a dielectric medium," J. Phys. B **39** S671 (2006).
10. S. M. Barnett, "Resolution of the Abraham-Minkowski dilemma," Phys. Rev. Lett. **104** 070401 (2010)
11. S. M. Barnett and R. Loudon, "The enigma of optical momentum in a medium," Phil. Trans. R. Soc. A **368** 927 (2010).
12. I. Brevik, "Experiments in phenomenological electrodynamics and the electromagnetic energy-momentum tensor," Phys. Rep. **52** 133 (1979).
13. R. Loudon, "Theory of the forces exerted by Laguerre-Gaussian light beams on dielectrics," Phys. Rev. A **68** 013806 (2003).
14. R. A. Beth, "Mechanical detection and measurement of the angular momentum of light," Phys. Rev. **50** 115 (1936).
15. L. Allen, M. J. Padgett, M. Babiker, "IV The orbital angular momentum of light," Prog. Opt. **39** 291 (1999).
16. J. D. Jackson, *Classical Electrodynamics*, 3rd ed. (John Wiley & Sons, New York, 1999).
17. J. B. Götte and M. R. Dennis, "Generalized shifts and weak values for polarization components of reflected light beams," New J. Phys. **14** 073016 (2012).
18. F. Goos and H. Hänchen, "Ein neuer und fundamentaler Versuch zur Totalreflexion," Ann. Phys., Lpz **436** 333 (1947).
19. R. Loudon, "Theory of the radiation pressure on dielectric surfaces," J. Mod. Opt. **49** 821 (2002).
20. R. Loudon, *The quantum theory of light*, 3rd ed. (Oxford University Press, Oxford, 2000).
21. A. Aiello, C. Marquardt, and G. Leuchs, "Transverse angular momentum of photons," Phys. Rev. A. **81** 053838 (2010).
22. K. J. Blow, R. Loudon, S. J. D. Phoenix and T. J. Shepherd, "Continuum fields in quantum optics," Phys. Rev. A. **42** 4102 (1990).
23. M. Abraham, "Zur elektrodynamik bewegter körper," Rend. Circ. Mat. Palermo **28** 1 (1909).
24. S. M. Barnett and P. M. Radmore, *Methods in Theoretical Quantum Optics*, (Oxford University Press, New York, 1997).
25. M. Padgett, S. M. Barnett and R. Loudon, "The angular momentum of light inside a dielectric," J. Mod. Opt. **50** 1555 (2003).
26. M. Kristensen and J. P. Woerdman, "Is photon angular momentum conserved in a dielectric medium?" Phys. Rev. Lett. **72** 2171 (1994).
27. M. Onoda, S. Murakami and N. Nagaosa, "Hall effect of light," Phys. Rev. Lett. **93** 083901 (2004).
28. K. Y. Bliokh, F. J. Rodriguez-Fortuno, F. Nori and A. V. Zayats, "Spin-orbit interaction of light," Nat. Photonics **9** 796 (2015).
29. J. M. Bennett, "A critical evaluation of rhomb-type quarterwave retarders," Appl. Opt. **9** 2123 (1970).
30. A. T. O'Neil, I. MacVicar, L. Allen, and M. J. Padgett, "Intrinsic and extrinsic of the orbital angular momentum of a light beam," Phys. Rev. Lett **88** 053601 (2002).
31. M. W. Beijersbergen, L. Allen, H. E. L. O. van der Veen, and J. P. Woerdman, "Astigmatic laser mode converters and transfer of orbital angular momentum," Opt. Commun. **96** 123 (1993).
32. M. J. Padgett and L. Allen, "Orbital angular momentum exchange in cylindrical-lens mode converters," J. Opt. B: Quantum Semiclass. Opt. **4** S17 (2002).